



## High contrast imaging on the THD bench: progress and upgrades

Raphaël Galicher, Pierre Baudoz, Jacques Robert Delorme, J. Mazoyer, Gérard Rousset, Josiane Firminy, Faouzi Boussaha, M. N'Diaye, Kjetil Dohlen, A. Caillat

### ► To cite this version:

Raphaël Galicher, Pierre Baudoz, Jacques Robert Delorme, J. Mazoyer, Gérard Rousset, et al.. High contrast imaging on the THD bench: progress and upgrades. Space Telescopes and Instrumentation 2014: Optical, Infrared, and Millimeter Wave, Jun 2014, Montréal, Quebec, Canada. pp.91435A 1-11, 10.1117/12.2055902 . hal-03804597

**HAL Id: hal-03804597**

**<https://hal.science/hal-03804597>**

Submitted on 13 Mar 2023

**HAL** is a multi-disciplinary open access archive for the deposit and dissemination of scientific research documents, whether they are published or not. The documents may come from teaching and research institutions in France or abroad, or from public or private research centers.

L'archive ouverte pluridisciplinaire **HAL**, est destinée au dépôt et à la diffusion de documents scientifiques de niveau recherche, publiés ou non, émanant des établissements d'enseignement et de recherche français ou étrangers, des laboratoires publics ou privés.

# PROCEEDINGS OF SPIE

[SPIDigitalLibrary.org/conference-proceedings-of-spie](https://spiedigitallibrary.org/conference-proceedings-of-spie)

## High contrast imaging on the THD bench: progress and upgrades

R. Galicher, P. Baudoz, J. R. Delorme, J. Mazoyer, G. Rousset, et al.

R. Galicher, P. Baudoz, J. R. Delorme, J. Mazoyer, G. Rousset, J. Firminy, F. Boussaha, M. N'Diaye, K. Dohlen, A. Caillat, "High contrast imaging on the THD bench: progress and upgrades," Proc. SPIE 9143, Space Telescopes and Instrumentation 2014: Optical, Infrared, and Millimeter Wave, 91435A (28 August 2014); doi: 10.1117/12.2055902

**SPIE.**

Event: SPIE Astronomical Telescopes + Instrumentation, 2014, Montréal, Quebec, Canada

# High contrast imaging on the THD bench: progress and upgrades

R. Galicher<sup>a</sup>, P. Baudoz<sup>a</sup>, J.R. Delorme<sup>a</sup>, J. Mazoyer<sup>a</sup>, G. Rousset<sup>a</sup>, J. Firminy<sup>b</sup>, F. Boussaha<sup>b</sup>, M. N'Diaye<sup>c</sup>, K. Dohlen<sup>d</sup>, A. Caillat<sup>d</sup>

<sup>a</sup>Lesia, Observatoire de Paris, CNRS, University Pierre et Marie Curie Paris 6, and University Denis Diderot Paris 7, 5 place Jules Janssen, 92195 Meudon, France;

<sup>b</sup>Gepi, Observatoire de Paris, CNRS, University Pierre et Marie Curie Paris 6, and University Denis Diderot Paris 7, 5 place Jules Janssen, 92195 Meudon, France;

<sup>c</sup>Space Telescope Science Institute, 3700 San Martin Drive, Baltimore, MD 21218, USA;

<sup>d</sup>Laboratoire d'Astrophysique de Marseille, Université d'Aix-Marseille & CNRS, UMR 7326, 38 rue Frédéric Joliot-Curie, 13388 Marseille Cedex 13, France;

## ABSTRACT

Direct imaging of exoplanets is very attractive but challenging and specific instruments like Sphere (VLT) or GPI (Gemini) are required to provide contrasts up to 16-17 magnitudes at a fraction of arcsec. To reach higher contrasts and detect fainter exoplanets, more-achromatic coronagraphs and a more-accurate wavefront control are needed. We already demonstrated contrasts of  $\sim 10^{-8}$  at  $\sim 4\lambda/D$  at 635nm using a four quadrant phase mask and a self-coherent camera on our THD bench in laboratory. In this paper, we list the different techniques that were tested on the THD bench in monochromatic and polychromatic lights. Then, we present the upgraded version of the THD bench that includes several deformable mirrors for correcting phase and amplitude simultaneously and obtain a field-of-view covering the complete 360 degrees arounds the star with contrasts down to  $\sim 10^{-8} - 10^{-9}$ .

**Keywords:** High contrast imaging, Exoplanets, Adaptive optics, Coronagraph, high angular resolution

## 1. INTRODUCTION

Since two decades, more than 1,800 exoplanets have been discovered using different techniques. Among these techniques, direct imaging is very attractive. It is the only one that can probe planets in the external part of their systems and provide a spectral characterization of their atmospheres. Unfortunately, direct imaging is challenging because of the large flux ratio (up to  $10^{10}$ ) and the small angular separation (fraction of arcsec) between the star and the planet. Thus, specific instruments like Sphere at VLT or GPI at Gemini were designed to study young giant gaseous exoplanets using photometry and spectroscopy in near-infrared. These instruments combine coronagraphs and an accurate control of the wavefront aberrations to detect sources up to 17 magnitudes fainter than their stars at a fraction of arcsec. To reach higher contrast levels with the next generation of instruments and thus, detect fainter (i.e. older or further) exoplanets, more achromatic coronagraphs and more accurate wavefront control systems will be needed. In this context, our team have been studying several high contrast imaging techniques for years at the Paris Observatory. To compare the techniques, we developed an optical high contrast imaging bench, called the THD bench. Using this laboratory bench, we have already demonstrated contrasts of  $\sim 10^{-8}$  at  $\sim 4\lambda/D$  in monochromatic light<sup>1</sup> at 635nm using a four quadrant phase mask<sup>2</sup> and a self-coherent camera<sup>1,3-6</sup> as reminded in §2. In §3, we describe other tests made on the THD bench to probe the chromatic performance of two others coronagraphs: a multi-stage four quadrant phase mask<sup>5</sup> or a dual zone phase mask.<sup>7</sup> In §4, we show the main laboratory results obtained on the THD bench when developing the multi-reference self-coherent camera that is a focal plane wavefront sensor working in polychromatic light. Finally, in §5, we present the on-coming upgrades of the THD bench that we started to implement to study the correction of both phase and amplitude aberrations simultaneously.

---

E-mail: raphael.galicher@obspm.fr

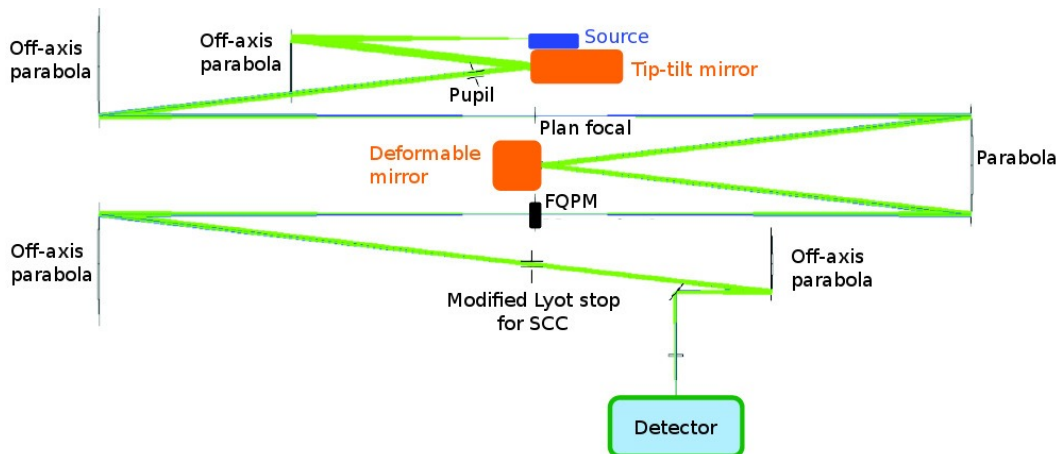


Figure 1. Optical layout of the THD bench.

## 2. OBJECTIVES AND PERFORMANCE OF THE THD BENCH

Direct imaging of exoplanets is challenging because a planet is  $10^4$  to  $10^{10}$  fainter than its hosting star and the angular separation between the two is a fraction of an arcsec. Thus, dedicated techniques are required to attenuate the stellar flux without affecting the exoplanetary image. A common configuration uses a coronagraph to reject as much stellar light as possible and a focal plane wavefront sensor to insure that wavefront aberrations are controlled. In the last decade, a lot of coronagraphs and several focal wavefront sensors have been proposed and it is often hard to compare the performance of all these devices as they are usually not tested under the same conditions. In this context, our team built an optical high contrast imaging testbed, called the THD bench, about eight years ago. The main objective is the comparison of high contrast imaging techniques under the same conditions to optimize the design of future instruments dedicated to direct imaging of exoplanets. At start, we developed the testbed using two techniques proposed by our team: a four quadrant phase mask (FQPM<sup>2</sup>) as coronagraph and a self-coherent camera (SCC<sup>3-5</sup>) as a focal plane wavefront sensor. The first version of the THD bench described in details in previous papers<sup>8,9</sup> was also composed of a tip-tilt mirror and a 32x32 BMC deformable mirror (Fig.1). The performance of the FQPM+SCC association are described in several papers.<sup>1,6,10</sup> Fig. 2 shows an image obtained in monochromatic light (left). The contrast in the dark hole (i.e. area of the image where we can minimize the speckle noise using the deformable mirror) is  $\sim 10^{-8}$  between 5 and  $12\lambda/D$ . Reaching such contrasts demonstrates the quality of THD bench optics in monochromatic light. However, the FQPM performance quickly degrades when broadening the spectral bandpass as seen in the 5% bandpass image (right) where bright speckles and Airy rings invade the dark hole. This behavior is expected as our FQPM device induces the required  $\pi$ -phase-shifts for a unique wavelength (640 nm).<sup>11</sup> That is why two more achromatic coronagraphs have been tested on the THD bench as described in the following section.

## 3. TESTS OF ACHROMATIC CORONAGRAPHS

The multi-FQPM (MFQPM<sup>12</sup>) and the dual zone phase mask (DZPM<sup>7</sup>) coronagraphs are phase coronagraphs that were proposed to mitigate the chromatic limitation of focal plane phase masks.

### 3.1 Multi-FQPM performance

The MFQPM uses several monochromatic FQPMs in cascade and it has been demonstrated in laboratory that it can attenuate the stellar flux down to a level of  $\sim 10^{-6}$  over a 20% bandpass.<sup>5</sup> In this previous work, the wavefront aberrations were not controlled and the performance was limited by the speckle noise. In this section, we present the performance of a MFQPM prototype that was tested on the THD bench.

First, we used the association of the SCC focal plane wavefront sensor with the MFQPM in monochromatic light to correct for the wavefront aberrations and create a dark hole in the image down to a  $\sim 3.10^{-8}$  level between

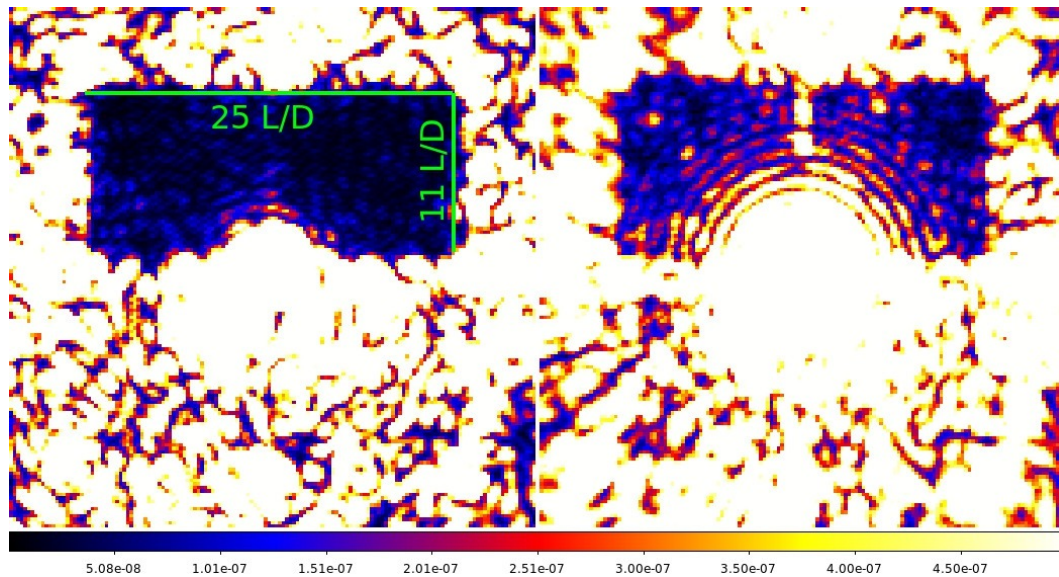


Figure 2. Laboratory images obtained on the THD bench using the association of a four quadrant phase mask and a self-coherent camera in monochromatic light (left) and with a 5% bandpass (right). The color scale is the same for both images.

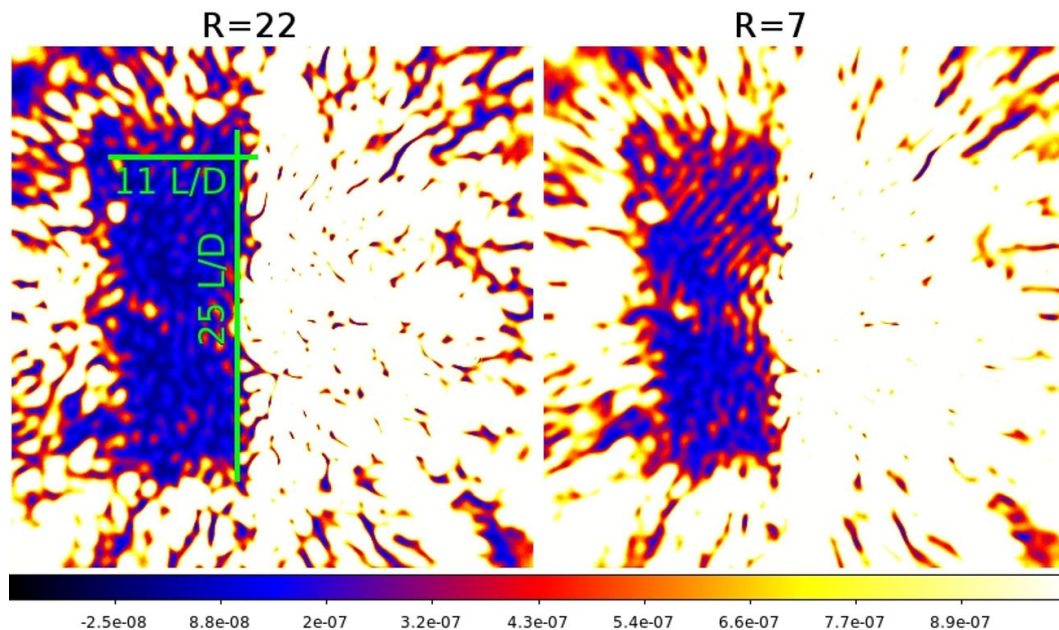


Figure 3. Laboratory images recorded behind a multi-four-quadrant phase-mask coronagraph on the THD bench using a 5% (left) or 14% (right) bandpass. The color scale is the same for both images.

5 and  $12\lambda/D$ .<sup>13</sup> The performance is thus very similar to the FQPM+SCC association. Then, we probed the chromatic behavior of the MFQPM recording the images using narrow (10 nm wide) and large (30 and 90 nm wide) filters. We found that the tested MFQPM is more achromatic than the FQPM but its performance is not as good as expected from numerical simulations. Indeed, the speckle intensity quickly increases when the filter gets larger (right image compared to left image in Fig. 3). As explained in Delorme et al (2014),<sup>13</sup> we conclude that one of the non-adjustable lenses of the MFQPM prototype was misaligned by construction.

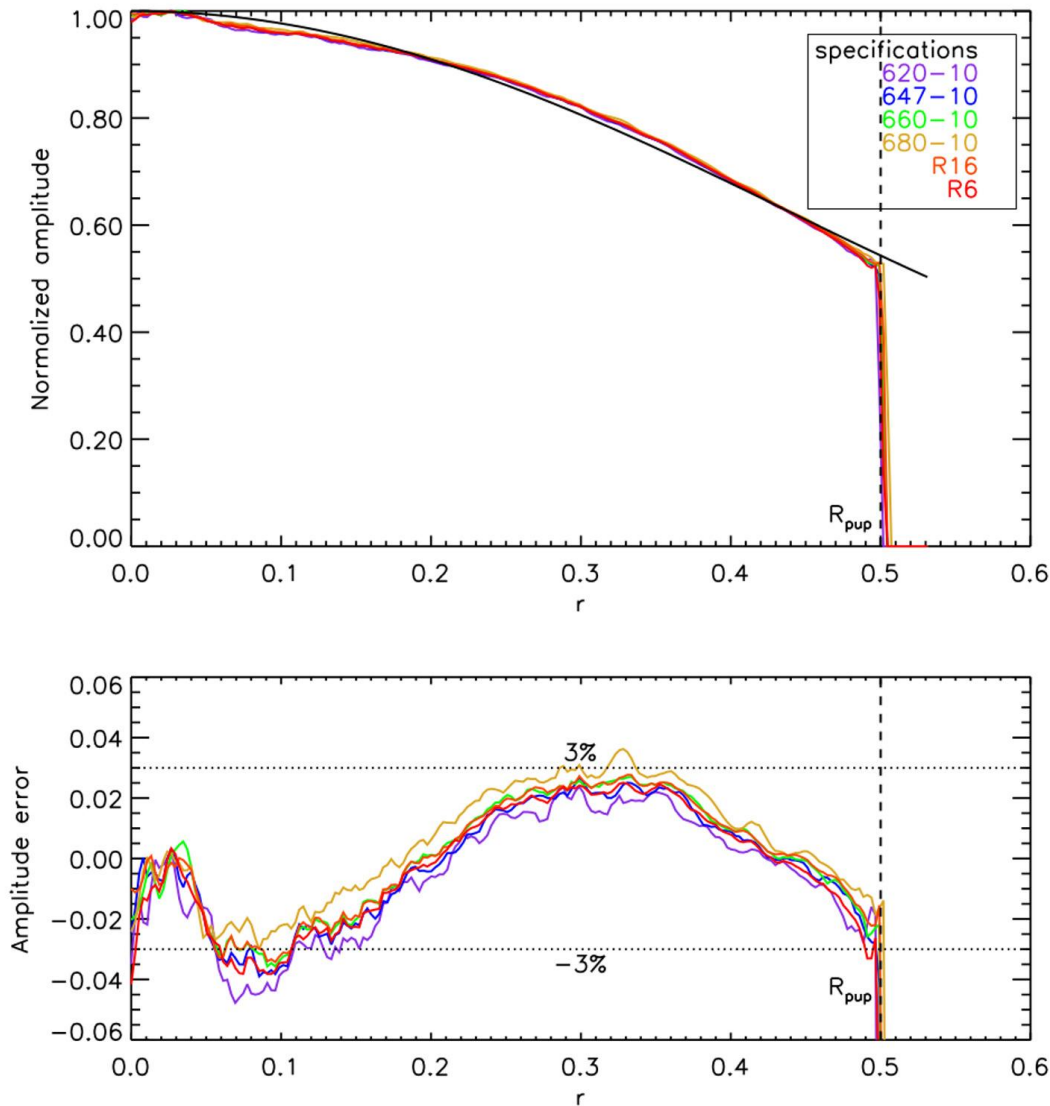


Figure 4. DZPM apodizer normalized transmission as a function of distance from the center of the pupil as measured on the THD bench (top) and the difference from the expected apodization function (bottom). The abscissa unit is the pupil radius. The transmission was measured at several 10 nm wide filters centered on 620 nm (purple), 647 nm (blue), 660 nm (green), and 680 nm (orange). It was also measured using filters of 5% (R16 orange curve) and 15% (R6 red curve).

### 3.2 Dual zone phase mask performance

The dual zone phase mask (DZPM) is an achromatized evolution of the Roddier&Roddier mask coronagraph.<sup>14</sup> It combines a shallow apodization of the pupil with a circularly symmetric mask pattern in the following focal plane that induces a double phase-shift of the stellar peak. From numerical simulations, the DZPM is expected to strongly attenuate the stellar light over a large bandpass<sup>15</sup> and a prototype was designed in order to reach  $\sim 10^{-8}$  contrast levels in visible light (600 to 700 nm) at a few resolution elements from the central star. Fig. 4 plots the radial profiles of the pupil apodizer manufactured by Actiwave as measured on the THD bench in several spectral filters (top) and the difference from the expected function (bottom). These plots confirm the device is in the specifications (deviation smaller than 3%). We also checked that the focal plane mask manufactured by Silios was in specifications by interferometric microscope measurements. Then, we probed the coronagraphic performance of the prototype on the THD bench.



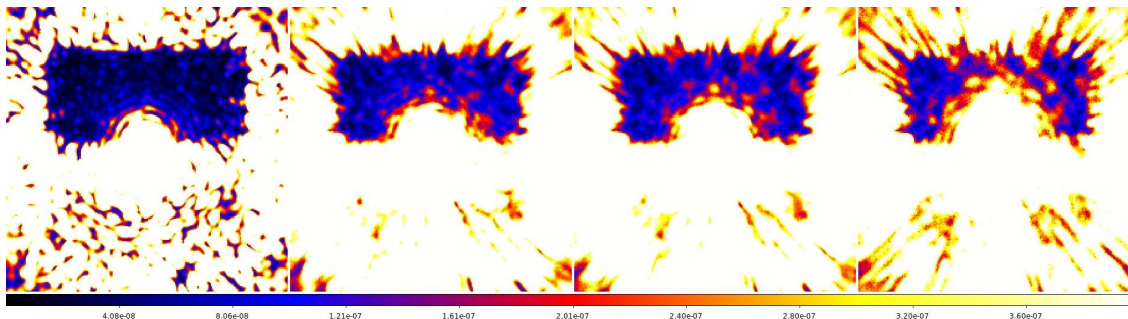


Figure 5. Laboratory images obtained with a dual zone phase mask coronagraph on the THD bench in white light using spectral filters of different widths: 40 nm, 200 nm, 250 nm, and 300 nm from left to right. The color scale is the same in all images.

The first test consisted of creating a dark hole in monochromatic light using a DZPM+SCC. After  $\sim 20$  iterations of the quasi-static speckle correction loop driven by the SCC at  $\sim 50$  Hz, the contrast inside the dark hole was  $\sim 10^{-8}$  as expected.<sup>13</sup> Then, we switched to a white-light source, applying several filters of different widths: 40 nm, 200 nm, 250 nm, and 300 nm (from left to right in Fig. 5). These images and the associated contrast curves given in Fig. 6 prove the DZPM prototype tested on the THD bench is achromatic enough to reach contrast levels down to  $\sim 4 \cdot 10^{-8}$  between 5 and  $12 \lambda/D$  over a bandpass up to 250 nm wide. The contrast curves are the azimuthal standard deviation calculated in rings of  $1 \lambda/D$  width. From these images and a more detailed study,<sup>13</sup> we can conclude that the DZPM prototype that we tested on the THD bench is a powerful coronagraph that strongly reduces the stellar light over a very wide bandpass (up to 250 nm wide).

#### 4. TEST OF AN ACHROMATIC FOCAL PLANE WAVEFRONT SENSOR

In the previous experiments (§3), the speckle intensity was minimized using a self-coherent camera (SCC) in monochromatic light and then, the deformable mirror shape was hold while the different filters were used to light the system. Doing so, the chromatic performance of the coronagraphs were tested independently from the wavefront sensor chromatic behavior. It was important to use this protocole because previous papers<sup>1,5,6</sup> emphasized the chromatic limitation of the SCC that can work in quasi-monochromatic light only ( $\lambda/\Delta\lambda > 20$ ). Recently,<sup>16</sup> our team proposed an upgrade of the SCC, called the multi-reference SCC, to make it less sensitive to chromatism. In this section, we briefly present the main results obtained with the multi-reference SCC whereas a complete study is presented in an other paper.<sup>13</sup>

The main result is showed in Figs. 7 and 8. The former figure is the dark hole that was created behind the DZPM prototype using the multi-reference SCC to control the deformable mirror in polychromatic light (80 nm width,  $\lambda/\Delta\lambda \sim 8$ ). The latter figure plots the associated contrast curve (full curve) compared to the monochromatic light curve (dashed curve). The contrast level inside the dark hole when correcting in polychromatic light is close to the contrast reached in monochromatic light. These two figures prove that the multi-reference SCC can efficiently minimize the speckle intensity inside a dark hole even for spectral bandwidths similar to bandwidths that are currently used in the high contrast imaging instruments like the SPHERE<sup>17</sup> and GPI<sup>18</sup> integral field spectrometers. In other words, the multi-reference SCC could be used to calibrate the non-common path aberrations in these instruments and thus, suppress the quasi-static speckles.

#### 5. FUTURE DEVELOPMENTS

As seen in all images presented in this paper, the speckle intensity is minimized in only half of the area that could be controlled by the deformable mirror. This is not due to the wavefront sensor that we use but to the presence of both phase and amplitude aberrations in the beam. Using one deformable mirror only means that when observing a star, we could probe only 180 degrees of the field-of-view in each image. Thus, at least two images would be needed to probe the complete neighborhood of the star. To observe the field-of-view covering the 360 degrees around the star in each image, we need to enlarge the dark hole in all directions around the

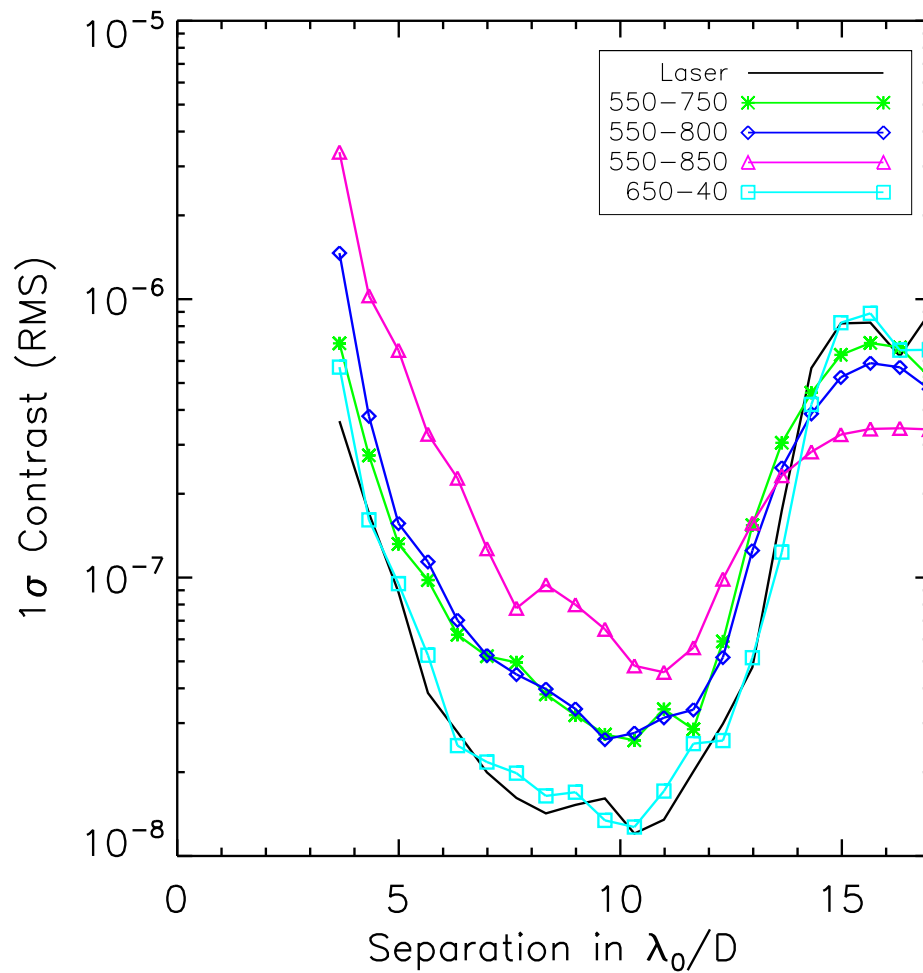


Figure 6. Contrast against angular separation derived from the images obtained with the dual zone phase mask in laser light (full black curve) and in white light using spectral filters of 40 nm (squares and light blue curve), 200 nm (star and green curve), 250 nm (diamonds and blue curve), and 300 nm (triangles and magenta curve) wide respectively.  $\lambda_0 = 640$  nm.



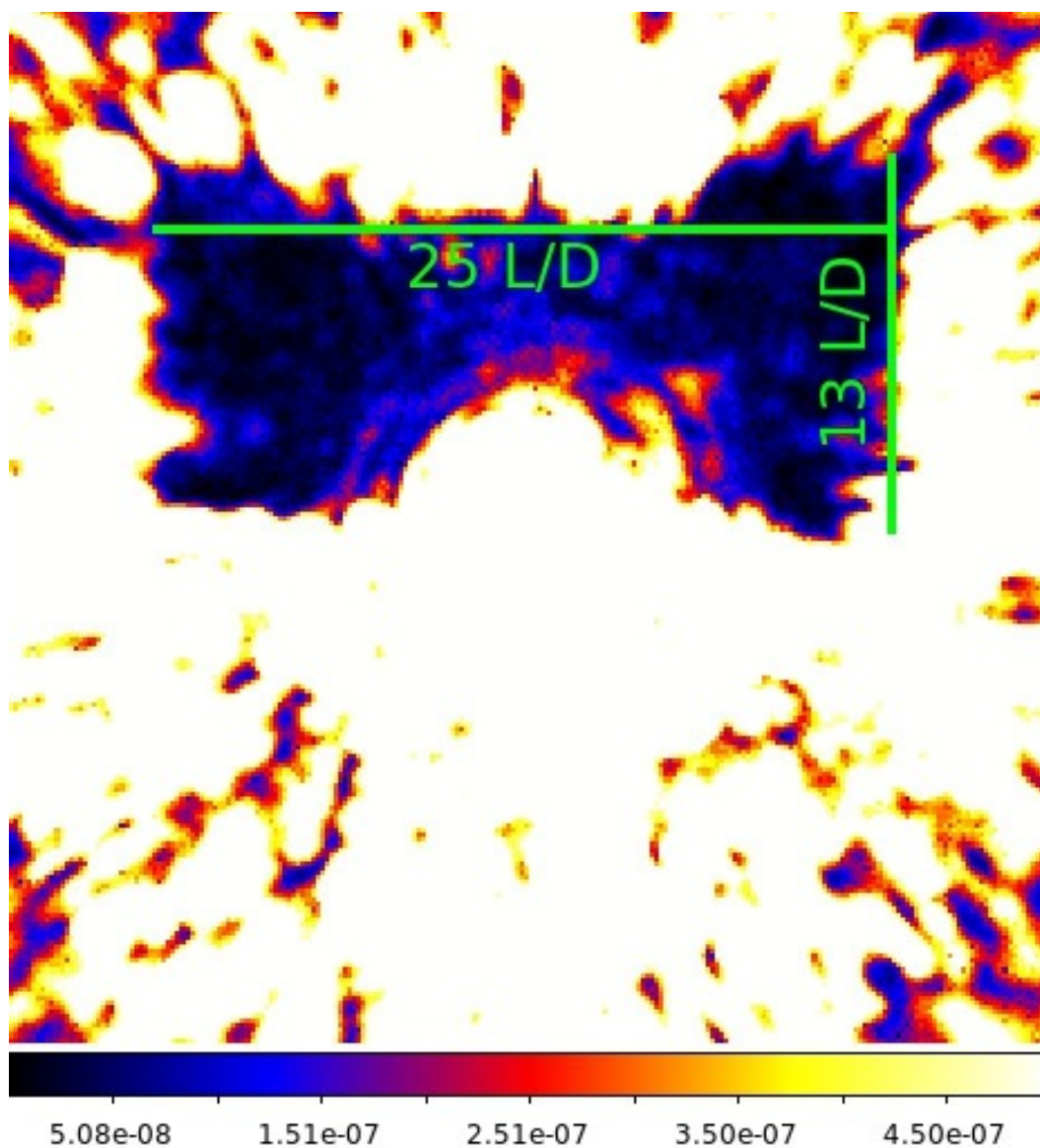


Figure 7. Laboratory image obtained on the THD bench using a multi-reference SCC to suppress the speckles inside the dark hole behind a DZPM coronagraph in polychromatic light ( $\lambda/\Delta\lambda \sim 8$ ).

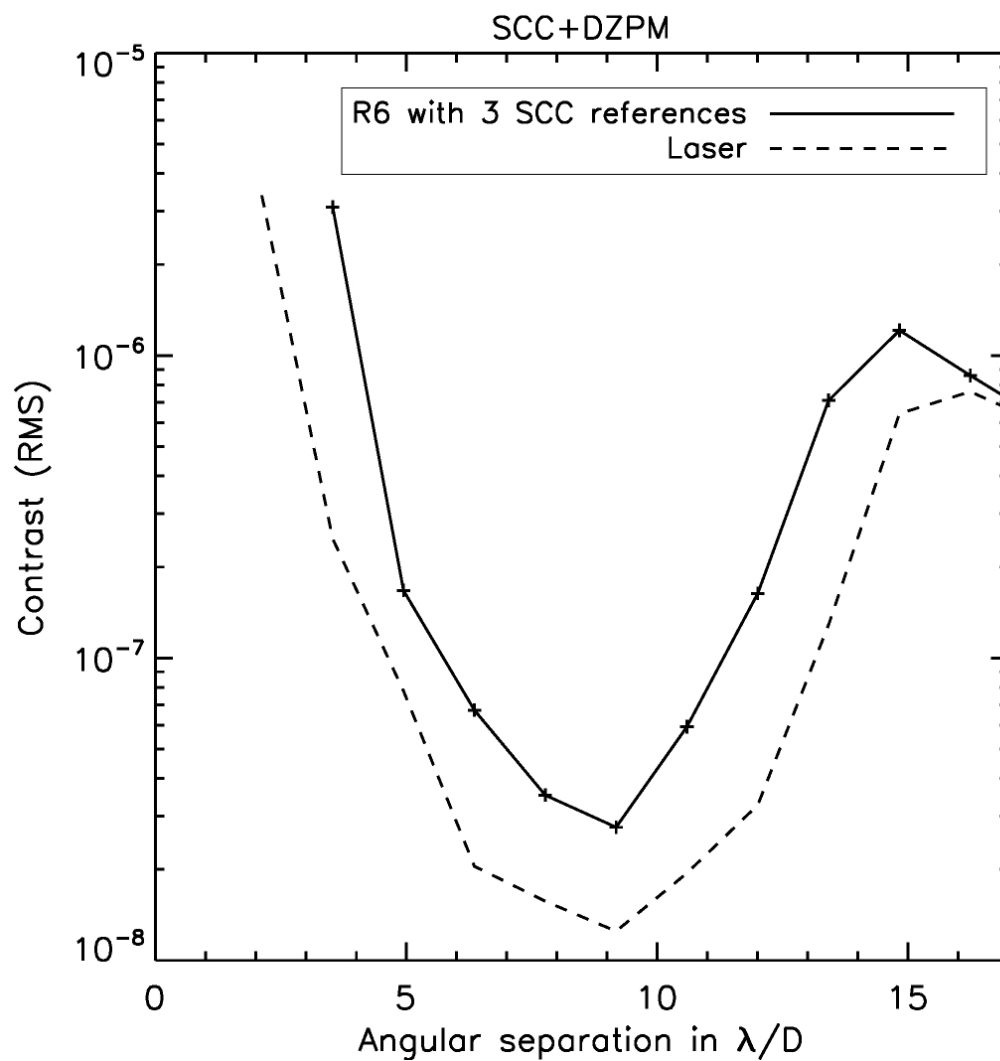


Figure 8. Contrast against angular separation derived from the images obtained with the association of a multi-reference SCC and a dual zone phase mask in laser light (dashed curve) and in white light using a 80 nm-wide bandpass ( $\lambda/\Delta\lambda \sim 8$ , full curve).

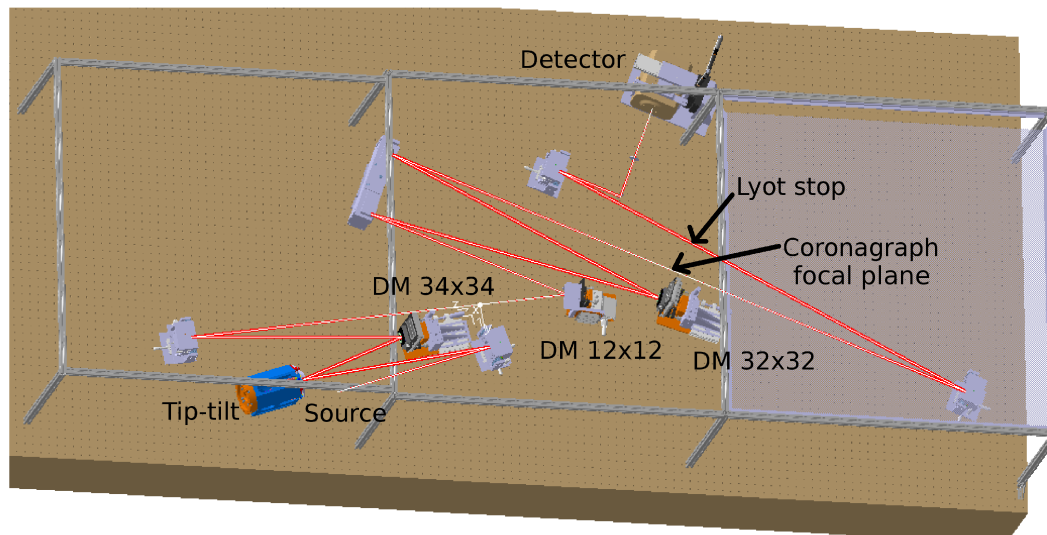


Figure 9. Layout of the upgraded THD bench composed of three deformable mirrors, one tip-tilt mirror, focal planes and pupil planes for implementing coronagraphs, apodizers and focal plane wavefront sensors.

star and this can be done only if we control both the phase and amplitude aberrations. In this context, we will upgrade the THD bench integrating two new deformable mirrors. Fig.9 presents the layout of the upgraded THD bench. We minimized the modifications from the previous version of the bench (Fig.1). The tip-tilt mirror and the parabola are the same. The bench still includes a coronagraph composed of a focal plane mask, a Lyot stop, and a possible pupil apodizer upstream from the focal plane mask. In the Lyot stop plane, we can add small off-axis holes to create a multi-reference self-coherent camera. The new features are a 34x34 and a 12x12 deformable mirrors. They will be set in out-of-pupil planes so that they can impact the amplitude of the wavefront in a following pupil plane because of Fresnel propagation. Doing so, we will be able to control both the amplitude aberrations with the 12x12 and 34x34 mirrors and the phase aberrations with the 32x32 mirror. The positions of the 12x12 and 34x34 mirrors will be optimized to correct for amplitude aberrations that induce speckles between 0 and  $16\lambda/D$  (32x32 mirror cut-off) in the image. Another new feature of the THD bench that is not represented in Fig.9 is an additional channel for the tip-tilt control. We will indeed use the reflected light in the outer part of the Lyot stop to accurately control the tip-tilt and possibly the low order aberrations as proposed by Singh et al (2014<sup>19</sup>).

## 6. CONCLUSIONS

We presented the main results obtained on the Paris Observatory THD bench, an optical high contrast imaging bench designed to study several techniques under the same conditions and to optimize their associations.

First, the THD bench was used to reach contrasts of  $\sim 10^{-8}$  at  $\sim 4\lambda/D$  in monochromatic light<sup>1</sup> at 635 nm using a four quadrant phase mask<sup>2</sup> as a coronagraph and a self-coherent camera<sup>1,3-6</sup> as a focal plane wavefront sensor. Then, the THD bench was used to probe the chromatic behavior of two coronagraphs. The multi-stage four quadrant phase mask<sup>5</sup> which performance in monochromatic light are similar to the four quadrant phase mask but that is less achromatic than expected because of an optical defect of the tested prototype. The second coronagraph was a dual zone phase mask that is very efficient in attenuating the stellar light in wide bands with a  $4.10^{-8}$  contrast level between 5 and  $12\lambda/D$  over a 250 nm bandpass ( $\lambda/\Delta\lambda \sim 3$ ). This last experiment proves that the dual zone phase mask has good performance in broadband but also that the THD bench has almost no chromatic aberrations.

The THD bench was also used to develop the self-coherence camera as a focal plane wavefront sensor.<sup>1,3-6</sup> The last upgrade of the technique make it work in visible light with a 80 nm bandpass as described in Delorme et al (2014).<sup>13</sup>

In June 2014, we started to upgrade the THD bench. We are integrating to more deformable mirrors to be able to control the phase and amplitude aberrations simultaneously and thus, create a dark hole in all directions around the star. In its upgraded version, the THD bench will stay versatile so that several techniques can be tested under the same conditions. We plan to test a vortex coronagraph<sup>20</sup> and other wavefront control techniques as the phase diversity adapted to coronagraphic images. We also stay open to new collaborations.

## REFERENCES

- [1] Mazoyer, J., Baudoz, P., Galicher, R., and Rousset, G., “High-contrast imaging in polychromatic light with the self-coherent camera,” *Astronomy & Astrophysics* **564**, L1 (Apr. 2014).
- [2] Rouan, D., Riaud, P., Boccaletti, A., Clénet, Y., and Labeyrie, A., “The four-quadrant phase-mask coronagraph. i. principle,” *Publications of the Astronomical Society of the Pacific* **112**, 1479–1486 (Nov. 2000).
- [3] Baudoz, P., Boccaletti, A., Baudrand, J., and Rouan, D., “The self-coherent camera: a new tool for planet detection,” in [*IAU Colloq. 200: Direct Imaging of Exoplanets: Science Techniques*], Aime, C. and Vakili, F., eds., 553–558 (2006).
- [4] Galicher, R., Baudoz, P., and Rousset, G., “Wavefront error correction and earth-like planet detection by a self-coherent camera in space,” *Astronomy and Astrophysics* **488**, L9–L12 (Sept. 2008).
- [5] Galicher, R., Baudoz, P., Rousset, G., Totems, J., and Mas, M., “Self-coherent camera as a focal plane wavefront sensor: simulations,” *Astronomy and Astrophysics* **509**, A31+ (Jan. 2010).
- [6] Mazoyer, J., Baudoz, P., Galicher, R., Mas, M., and Rousset, G., “Estimation and correction of wavefront aberrations using the self-coherent camera: laboratory results,” *Astronomy & Astrophysics* **557**, A9 (Sept. 2013).
- [7] Soummer, R., Dohlen, K., and Aime, C., “Achromatic dual-zone phase mask stellar coronagraph,” *Astronomy and Astrophysics* **403**, 369–381 (May 2003).
- [8] Mas, M., Baudoz, P., Rousset, G., Galicher, R., and Baudrand, J., “Self-coherent camera: first results of a high-contrast imaging bench in visible light,” in [*Society of Photo-Optical Instrumentation Engineers (SPIE) Conference Series*], *Society of Photo-Optical Instrumentation Engineers (SPIE) Conference Series* **7735** (July 2010).
- [9] Mas, M., Baudoz, P., Rousset, G., and Galicher, R., “Tip-tilt estimation and correction using FQPM coronagraphic images,” *Astronomy & Astrophysics* **539**, A126 (Mar. 2012).
- [10] Baudoz, P., Mazoyer, J., Mas, M., Galicher, R., and Rousset, G., “Dark hole and planet detection: laboratory results using the self-coherent camera,” in [*Society of Photo-Optical Instrumentation Engineers (SPIE) Conference Series*], *Society of Photo-Optical Instrumentation Engineers (SPIE) Conference Series* **8446** (Sept. 2012).
- [11] Baudoz, P., Boccaletti, A., Riaud, P., Cavarroc, C., Baudrand, J., Reess, J.-M., and Rouan, D., “Feasibility of the four-quadrant phase mask in the mid-infrared on the james webb space telescope,” *Publications of the Astronomical Society of the Pacific* **118**, 765–773 (2006).
- [12] Baudoz, P., Galicher, R., Baudrand, J., and Boccaletti, A., “Theory and laboratory tests of the multi-stage phase mask coronagraph,” in [*Society of Photo-Optical Instrumentation Engineers (SPIE) Conference Series*], *Presented at the Society of Photo-Optical Instrumentation Engineers (SPIE) Conference* **7015** (July 2008).
- [13] Delorme, J., Galicher, R., Baudoz, P., Rousset, G., Mazoyer, J., N’Diaye, M., and Dohlen, K., “High contrast imaging in wide spectral band with a self-coherent camera and achromatic coronagraphs,” in [*Society of Photo-Optical Instrumentation Engineers (SPIE) Conference Series*], *Presented at the Society of Photo-Optical Instrumentation Engineers (SPIE) Conference* **9151** (June 2014).
- [14] Roddier, F. and Roddier, C., “Stellar coronagraph with phase mask,” *Publications of the Astronomical Society of the Pacific* **109**, 815–820 (July 1997).
- [15] N’diaye, M., Dohlen, K., Cuevas, S., Soummer, R., Sánchez-Pérez, C., and Zamkotsian, F., “Improved achromatization of phase mask coronagraphs using colored apodization,” *Astronomy and Astrophysics* **538**, A55 (Feb. 2012).

- [16] Galicher, R., Delorme, J. R., Baudoz, P., and Mazoyer, J., “Focal Plane Wavefront Sensing with a self-coherent camera,” in [*Proceedings of the Third AO4ELT Conference*], Esposito, S. and Fini, L., eds. (Dec. 2013).
- [17] Beuzit, J.-L., Feldt, M., Dohlen, K., Mouillet, D., Puget, P., Wildi, F., Abe, L., Antichi, J., Baruffolo, A., Baudoz, P., Boccaletti, A., Carbillet, M., Charton, J., Claudi, R., Downing, M., Fabron, C., Feautrier, P., Fedrigo, E., Fusco, T., Gach, J.-L., Gratton, R., Henning, T., Hubin, N., Joos, F., Kasper, M., Langlois, M., Lenzen, R., Moutou, C., Pavlov, A., Petit, C., Pragt, J., Rabou, P., Rigal, F., Roelfsema, R., Rousset, G., Saisse, M., Schmid, H.-M., Stadler, E., Thalmann, C., Turatto, M., Udry, S., Vakili, F., and Waters, R., “SPHERE: a planet finder instrument for the VLT,” in [*Society of Photo-Optical Instrumentation Engineers (SPIE) Conference Series*], *Society of Photo-Optical Instrumentation Engineers (SPIE) Conference Series* **7014** (Aug. 2008).
- [18] Macintosh, B. A., Graham, J. R., Palmer, D. W., Doyon, R., Dunn, J., Gavel, D. T., Larkin, J., Oppenheimer, B., Saddlemyer, L., Sivaramakrishnan, A., Wallace, J. K., Bauman, B., Erickson, D. A., Marois, C., Poyneer, L. A., and Soummer, R., “The Gemini Planet Imager: from science to design to construction,” in [*Society of Photo-Optical Instrumentation Engineers (SPIE) Conference Series*], *Society of Photo-Optical Instrumentation Engineers (SPIE) Conference Series* **7015** (July 2008).
- [19] Singh, G., Guyon, O., Baudoz, P., Jovanovic, N., Martinache, F., Kudo, T., Serabyn, E., and Kuhn, J. G., “Lyot-based Low Order Wavefront Sensor: Implementation on the Subaru Coronagraphic Extreme Adaptive Optics System and its Laboratory Performance,” *Submitted* (June 2014).
- [20] Mawet, D., Riaud, P., Absil, O., and Surdej, J., “Annular groove phase mask coronagraph,” *The Astrophysical Journal* **633**, 1191–1200 (Nov. 2005).